Fight not flight: parasites drive the bacterial evolution of resistance, not avoidance

Michael Blazanin, Jeremy Moore, Sydney Olsen, and Michael Travisano

Abstract

In the face of ubiquitous threats from parasites, hosts often evolve strategies to resist infection or to altogether avoid contact with parasites. At the microbial scale, bacteria frequently encounter viral parasites, bacteriophages. While bacteria are known to utilize a number of strategies to resist infection by phages, and can physically navigate their environment using complex motility behaviors, it is unknown whether bacteria evolve avoidance of phages. In order to answer this question, we combined experimental evolution and mathematical modeling. Experimental evolution of the bacterium *Pseudomonas fluorescens* in environments with differing spatial distributions of the phage Phi2 revealed that the host bacteria evolved resistance depending on parasite distribution and infectivity, but did not evolve dispersal to avoid parasite infection. Simulations using parameterized mathematical models of bacterial growth and swimming motility showed that this is a general finding: while increased dispersal is adaptive in the absence of parasites, in the presence of parasites that fitness benefit disappears and resistance becomes adaptive, regardless of the spatial distribution of parasites. Together, these experiments suggest that parasites should rarely, if ever, drive the evolution of bacterial avoidance via dispersal.

Introduction

In nature, organisms have numerous evolutionary responses to the ubiquitous threats they face from parasites. One common strategy is resistance, where defenses prevent the establishment and proliferation of parasites (Hall et al. 2017; Gibson and Amoroso 2022). However, another strategy is avoidance, which precludes infection by reducing the rate of contact between hosts and parasites in the first place (Gibson and Amoroso 2022). In fact, examples of parasite avoidance are common. For instance, the presence of parasitoid wasps causes aphids to produce more highly-dispersing offspring (Sloggett and Weisser 2002), and the presence of parasites induces greater dispersal in back-swimmers (Baines et al. 2020), *Drosophila* (Brophy and Luong 2021), and freshwater protists (Zilio et al. 2021).

One domain where host-parasite interactions are extremely common is that of microbes. In particular, bacteria and their viral parasites, bacteriophages, are the two most abundant biological entities on the planet (Whitman et al. 1998; Hendrix et al. 1999; Bar-On et al. 2018; Mushegian 2020). When a phage infects a bacterial cell, it co-ops the cellular machinery to replicate, often harming or killing the host. This host-parasite interaction between bacteria and phages has major effects, from the global ecosystem (Finlay et al. 1997; Whitman et al. 1998; Wommack and Colwell 2000; Weitz and Wilhelm 2012) to human health (Kortright et al. 2019).

In the face of constant threats from phages, bacteria have been found to utilize a number of strategies to resist infection by phages (Hampton et al. 2020). For instance, bacterial populations can evolve resistance by modifying the cellular structures that phages rely on, especially the extracellular structures used by phages to initially attach to the cell. Bacteria can also carry any number of cytoplasmic defenses that operate after a phage infects the cell. In fact, bacteria can even activate intracellular defenses in response to signals from phage-infected neighbors (de Mattos et al. 2022). Moreover, recent advancements have revealed an enormous diversity of previously-undiscovered defense systems (Millman et al. 2020, 2022), suggesting that many more bacterial responses to phages remain to be found.

While bacterial resistance to phages has been extensively studied, bacterial avoidance of phages has not. Many bacteria do have complex motility behaviors that they use to disperse and physically navigate their environment (Wadhwa and Berg 2022). For instance, bacteria can detect a number of attractant and repellant signals. They also have several mechanisms for motility, including tail-like flagella that enable swimming or swarming in liquid and semi-solid environments, pili for twitching motility on surfaces, and extracellular adhesions for gliding across surfaces (Wadhwa and Berg 2022). However, while the molecular mechanisms of many of these systems are well-established, the ecological functions they fulfill in natural environments, including whether they enable avoidance of phages, often remain unresolved (Keegstra et al. 2022).

To our knowledge, there are no examples of bacteria evolving dispersal to avoid phage infection (Keegstra et al. 2022), and it is unclear whether, or to what degree, the evolution of bacterial dispersal can be driven by phages. Some compelling work has indirectly tested this idea in spatially structured environments. For instance, Li et al and Taylor & Buckling carried out studies on dispersing bacteria and phages. Their ecological data supported the evolutionary prediction that phages could select for bacteria with greater dispersal (Taylor and Buckling 2013; Li et al. 2020). In contrast, the ecological and evolutionary experiments of Ping et al. implied that the presence of phages should select for resistance

and not dispersal (Ping et al. 2020). Here, we carry out the first direct test of the hypothesis that bacteria can evolve dispersal to avoid phages.

To test this hypothesis, we manipulate the distribution of parasites in space, which is predicted to alter the evolution of bacterial resistance and avoidance. For instance, selection for resistance strengthens with spatial homogeneity and parasite spread (Brockhurst et al. 2003; Vogwill et al. 2008), while selection for avoidance strengthens as the local risk of infection or spatial heterogeneity of the environment increase (Boulinier et al. 2001; Weisser 2001; Baines et al. 2020). Here, we manipulate the spatial distribution of phages to leverage those effects and test whether bacteria can evolve to avoid phages. Combining experimental evolution and mathematical modeling approaches, our findings suggest that bacterial avoidance of phages by dispersal is not evolutionarily favored over resistance.

Materials & Methods

Bacteria & Phage Strains and Culturing

We used the widely-studied model system of *P. fluorescens* SBW25 and its strictly-lytic phage Phi2 (Brockhurst et al. 2007), which putatively binds the bacterial lipopolysaccharide (LPS) (Scanlan and Buckling 2012). We used variations of King's B (KB) medium (the standard SBW25 bacterial media, see experimental evolution section below): 10 g/L LP0037 Oxoid Bacteriological Peptone, 15 g/L glycerol, 1.5 g/L potassium phosphate, and 0.6 g/L magnesium sulfate. Amplified phage stocks were created by infecting an actively growing SBW25 liquid culture, incubating while shaking for 24 hours at 28°C, then adding 25 µL chloroform per mL culture and storing at 4°C.

Measuring Phage & Bacterial Density

Phage and bacterial concentrations were quantified using standard plating and optical density measurements. Phages were quantified in plaque-forming-units per mL (PFU/mL) using a plaque assay: phage suspensions and 100 µL of an overnight bacterial culture in the appropriate KB concentration were added to 4 mL of 0.5% agar KB media at 45°C then poured over 1.5% agar KB plates. After overnight incubation at 28°C plaque forming units were counted. Bacteria were quantified by plating serial dilutions onto 1.5% agar KB plates and counting the number of colony-forming-units (CFU). In liquid culture, bacterial density was quantified by measuring the optical density at 600 nanometers (OD600) with a spectrophotometer, then translating that to CFU/mL using a previously-established standard curve.

Experimental Evolution

Experimental evolution was conducted in plates containing media with 3 g/L agar. Each of the three parasite distribution treatments (Fig 1) was carried out in two different growth conditions, which differed in the degree of phage replication ("weak phage" and "strong phage"). For weak phage conditions, incubation was done at 30°C; for strong phage conditions, incubation was done at 29°C. Previous characterization of the temperature dependence of Phi2 growth shows that these two

temperatures have a strong effect on phage replication, with a much smaller effect on *P. fluorescens* growth (Padfield et al. 2019).

Bacteria growing in media with 3 g/L agar can disperse via swarming or swimming motility (Kohler et al. 2000; Harshey 2003). For experimental tractability, nutrient concentrations in the media were altered to prevent the formation of swarms. At each temperature, we tested KB formulations with 3 g/L agar, either 25%, 50%, 75%, or 100% concentrations of glycerol and peptone (the carbon and nitrogen sources), and 50% concentrations of potassium phosphate and magnesium sulfate. We then selected the highest-nutrient formulation that did not induce bacterial swarming. For weak phage conditions, that was "50%/50% KB". For strong phage conditions, we used "25%/50% KB".

The day before inoculation or passage, 25 mL of media was poured into each plate with an internal diameter of 90 mm. For the global parasite treatment, media was cooled to 50°C and Phi2 was added before pouring to reach a final phage concentration of 10^6 PFU/mL. T0 inoculations were taken from an exponentially growing culture of ancestral *P. fluorescens* that had been shaken at 250 rpm in the appropriate media. For the control and global treatments, 5 µL of a bacterial suspension with 5 x 10^7 CFU/mL was spotted onto the center of the plate. For the local treatment, 5 µL of a mixture containing 5 x 10^7 CFU/mL bacteria and 5 x 10^6 PFU/mL phages was spotted onto the center of the plate. These concentrations were chosen to that the initial inoculum droplet of bacteria would be exposed to approximately the same number of phages between the local and global treatments.

After bacteria are inoculated in the center of the plate, nutrient consumption creates a spatial gradient in chemoattractants. This gradient induces bacterial dispersal from the center of the plate towards the periphery, primarily via flagella-driven swimming. Thus, population-level dispersal is the result of both bacterial growth and motility (Fraebel et al. 2017). In these conditions, Phi2 only passively diffuses (Sampedro et al. 2015).

After initial inoculation, populations were then propagated to a new set of plates daily for 14 transfers, while re-creating the same phage spatial distribution each time. After ~24 hours incubation, a 300 µL pipette tip set to 5 µL was stabbed into the agar immediately past the visible cell front and drawn up slowly, to ensure no bubbles entered the tip. This 5 µL sample was then spotted onto the center of a new plate. Note that this imposes a narrow population bottleneck at each transfer. For the global treatment, plates were poured in the same manner as initial inoculations. For the local treatment, 2.5 µL of a phage stock with 10^7 PFU/mL was added onto the 5 µL droplet on the new plate, yielding the same area-density as the initial inoculations. After 14 transfers, evolved isolates were taken by spreading diluted suspensions of the 5 µL sample onto 1.5% agar KB plates and incubating for 48 hours.

Evolution populations were blocked such that each block contained one population in each of the control, local, and global treatments. Additionally, experimental evolution in weak phage and strong phage conditions were conducted separately, so comparisons should only be made within each condition. In some cases, plates showed no growth after 24 hours of incubation. In these cases, all three population in the block were re-inoculated from the previous transfer, which had been stored at 4°C. This occurred seven times (Table S1), predominantly in the first two transfers, when phage killing was

most frequent. Additionally, one global and one local population, both under the weak phage condition, became contaminated during the experiment and were excluded from analysis.

Quantifying Bacterial Dispersal/Growth in Soft Agar

Bacterial growth during experimental evolution was quantified the same way as dispersal (sometimes called 'migration rate') of evolved bacterial isolates. For experimental evolution, plates were photographed at 300 dpi immediately before passaging. To characterize evolved isolates, 5 µL of a bacterial suspension at $5x10^7$ CFU/mL was spotted onto the center of a 25mL 0.3% agar plate of the appropriate media, then incubated for approximately 24 hours before photographing at 300 dpi. All plates from a given experimental block were poured from the same bottle of media the day before inoculation. The area of the circular bacterial growth in these images was measured manually using Fiji (Schindelin et al. 2012). Then, this area was normalized for the exact time of incubation under the assumption that radius increases linearly with time (Croze et al. 2011). For evolved isolates, the dispersal rate of a plate containing the ancestral bacteria incubated the same day was subtracted to reduce batch effects and produce the delta dispersal value.

Quantifying Bacterial Resistance to Phage

Bacterial resistance to phage was quantified using an efficiency of plaquing assay. A phage stock was quantified simultaneously on a lawn of the ancestral bacteria and evolved isolates, and the ratio of the titer of each isolate relative to the average of triplicate titers on the ancestral bacteria was calculated.

Quantifying Bacterial Growth in Liquid

To quantify bacterial growth in liquid, 4 µL of an overnight bacterial culture was added, in duplicate wells, to 146 µL of media in each well of a 96-well plate. Media included both the media experimental evolution was carried out in ("Original"), and media with the concentrations of all components doubled from that ("Rich"). This plate was shaken and incubated at the appropriate temperature overnight, with the OD600 read every 15 or 30 minutes.

Then, growth curve data was computationally characterized using gcplyr (Blazanin 2023) and fitting to determine isolates' lag time, maximum per-capita growth rate (r), and density and time when a diauxic shift was observed (k, k_t). The first half hour of data points were noisy, so they were excluded. Then, data was smoothed using a moving median of 3 points, followed by LOESS smoothing with a span of either 1 hour or 6.94 hours. We identified the exponential start of logistic growth as the first point when the per-capita growth rate of the of the 1 hour LOESS-smoothed data exceeded 0.5/hour, or 0.4/hour when 0.5 was never reached. We identified the end of logistic growth as the first local minima in the derivative of the 6.94 hour LOESS-smoothed data. These criteria were manually verified as yielding time spans where the data reflected logistic growth, excluding any acclimation period at the beginning of the data, and any post-diauxic shift growth at the end of the data.

We then fit the data in the logistic growth window with a differential equation for logistic growth that was modified to have a deceleration parameter (Baranyi and Roberts 1994; Ram et al. 2019) (Equation

1). Here, N(t) denotes the density of bacteria at time t, r is the maximum per-capita growth rate, k is the carrying capacity, and v is the deceleration curve parameter.

$$\frac{dN}{dt} = rN\left(1 - \left(\frac{N}{k}\right)^{v}\right) \quad [1]$$

This differential equation has a closed-form solution (Ram et al. 2019) (Equation 2).

$$N(t) = \frac{k}{\left(1 - \left(1 - \left(\frac{k}{N_0}\right)^{v}\right)e^{-rvt}\right)^{\frac{1}{v}}} \quad [2]$$

Equation 2 was fitted to the raw unsmoothed data points in the logistic growth window. We then manually evaluated all wells with high fit error, excluding wells where the fit was poor. We extracted fitted maximum per-capita growth rates (r) and excluded any isolates where the standard deviation of r between technical replicates was greater than 0.12/hr (for weak phage conditions) or 0.14/hr (for strong phage conditions).

Statistical Analysis

All analyses and visualization were carried out in R 4.2.2 (R Core Team 2022) and RStudio 2022.12.0+353 using packages reshape (Wickham 2007), tidyr (Wickham et al. 2023*b*), dplyr (Wickham et al. 2023*a*), ggplot2 (Wickham 2016), ggh4x (Brand 2022), lme4 (Bates et al. 2015), pbkrtest (Halekoh and Højsgaard 2014), gcplyr (Blazanin 2023), cowplot (Wilke 2020), ggrepel (Slowikowski 2022), ggtext (Wilke and Wiernik 2022), magrittr (Bache and Wickham 2022), and purr (Wickham and Henry 2023), along with the Okabe and Ito colorblind-friendly palette (Okabe and Ito 2008). Any other statistical functions, like prcomp, were built-in to R. See https://github.com/mikeblazanin/trav-phage for all analysis code.

Simulations

To simulate bacterial dispersal with different parasite spatial distributions, we modified the widely-used Patlak-Keller-Segel model of bacterial chemotaxis and growth (Patlak 1953; Keller and Segel 1970) to include phage populations (Eqs. 3 – 6). These models have been previously validated to recreate *in vitro* bacterial population behavior with great precision (Cremer et al. 2019; Li et al. 2020; Ping et al. 2020; Mattingly and Emonet 2022).

$$\frac{dN}{dt} = \nabla(D_N \nabla N - \chi N \nabla A) + c_R Y \frac{R}{R+K_R} N - iNP \quad [3]$$

$$\frac{dP}{dt} = D_P \nabla^2 P + i(b-1)NP \quad [4]$$

$$\frac{dR}{dt} = D_R \nabla^2 R - c_R \frac{R}{R+K_R} N \quad [5]$$

$$\frac{dA}{dt} = D_A \nabla^2 A - c_A \frac{A}{A+K_A} N \quad [6]$$

In this model we track the population density of hosts (N), parasites (P), resources (R), and attractants (A) through both space and time, using parameters as defined in Table 1. Simulations were initiated with parasites excluded (Control), gaussian distributed about the origin (peak height = $5x10^8$ parasites/um, sd = $20um$) (Local), or uniformly distributed (2.5 parasites/um) (Global).

To assess the fitness landscape between resistance (i) and dispersal (χ), growth rate (c_R), attractant consumption (c_A), or yield (Y), the host population was split into two equally-sized sub-populations that shared the same initial distribution. One sub-population (the resident) had the parameter values listed in Table 1, while the other (the invader) had one or two parameter values which differed from the resident. Following this setup, the simulation was run for 20 simulated hours. At the end of the simulation, the fitness of the invader was calculated as $\log_{10}$(invader frequency/resident frequency). All models were implemented in Matlab (Mattingly and Emonet 2022) and all code is available at https://github.com/jeremymoore558/ks_phage. Visualization code is available at https://github.com/mikeblazanin/trav-phage.

Table 1. Parameters and values used in simulations.

Parameter	Description	Resident Value
D_N	Diffusion coefficient for bacteria	50 $\mu m^2/s$
D_P	Diffusion coefficient for phage	0 $\mu m^2/s$
D_R	Diffusion coefficient for resource	800 $\mu m^2/s$
D_A	Diffusion coefficient for attractant	800 $\mu m^2/s$
χ	Chemotactic sensitivity coefficient	315 $\mu m^2/s$
c_R	Uptake rate of resource	2.25×10^{-14} mmol/cfu/s
c_A	Uptake rate of attractant	4.17×10^{-16} mmol/cfu/s
Y	Cell yield	1.229×10^{10} cfu/mmol
K_R	Michaelis-Menten constant for resource	5×10^{-5} mmol/mL
K_A	Michaelis-Menten constant for attractant	1×10^{-6} mmol/mL
i	Infection rate	1×10^{-12} infec/cell/mL/pfu/mL/s
b	Number of parasites produced per infection	30 pfu/infec

Results

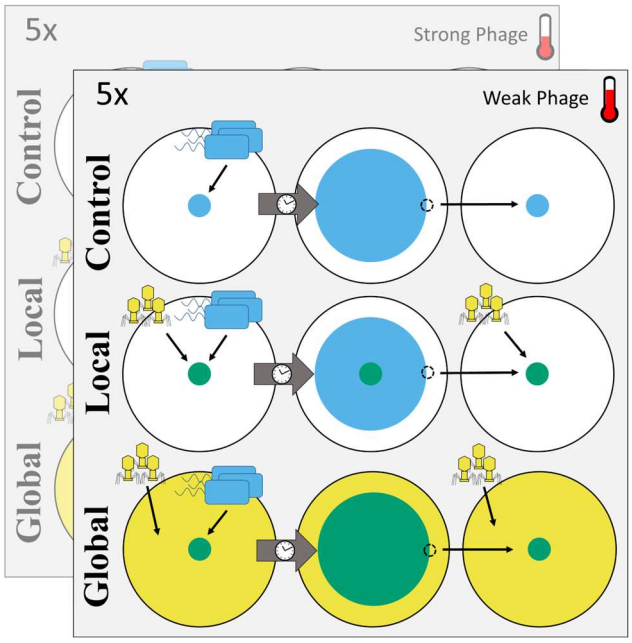

Figure 1. Experimental evolution design. Bacteria were inoculated into the center of an agar plate containing one of three treatments: phages excluded (control), phages only in the center of the plate (local), or phages throughout the plate (global). After 24 hours of incubation, bacteria (blue) have actively dispersed outwards, and a sample was taken from the cell front and transferred to the center of a new plate containing phages in the same distribution. Five evolutionary replicates were carried out for each treatment in each of two conditions: 29 °C, where the phages strongly replicate, and 30°C, where the phages only weakly replicate.

Bacterial Growth During Experimental Evolution

To test how parasite spatial distribution alters host evolution, we experimentally evolved *P. fluorescens* for approximately 350 generations in three treatments differing in their spatial distribution of parasites (Fig 1). This experiment was repeated under incubation and media conditions enabling strong or weak phage growth. After each day, the radius of bacterial growth was measured (Fig 2). We observed transient suppression of bacterial growth during the initial experimental evolution transfers in treatments containing phages (local and global). This pattern is consistent with initially high rates of phage predation on bacteria, which weakens following host evolution.

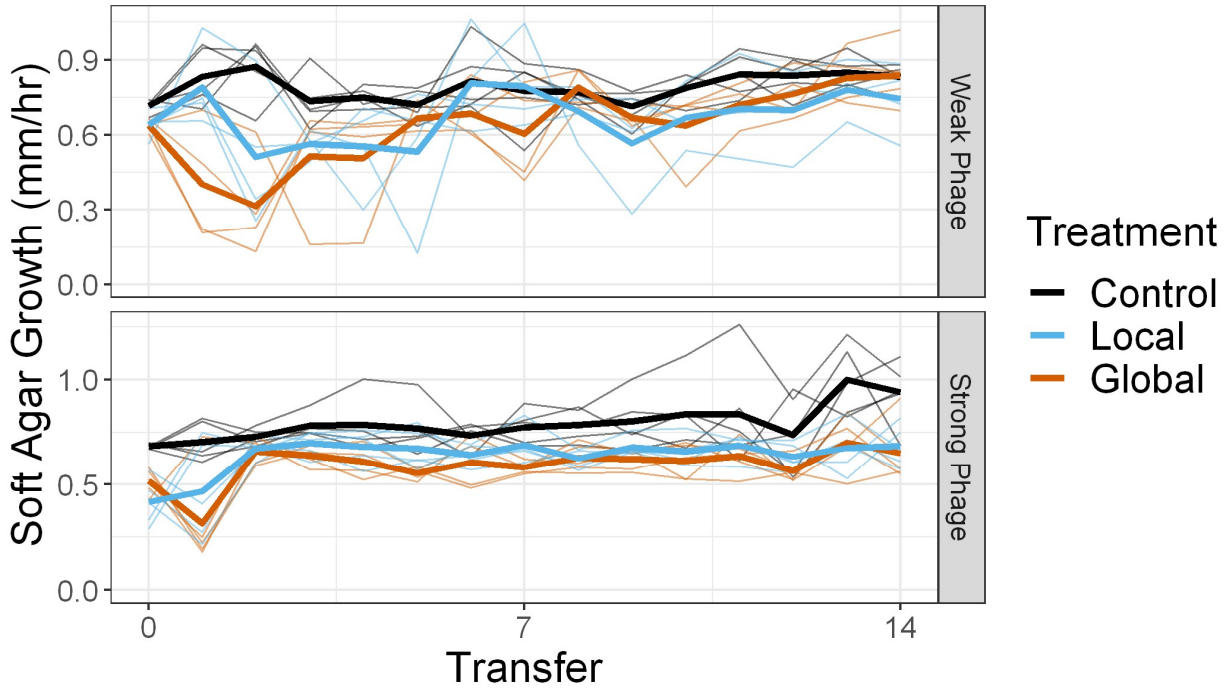

Figure 2. Bacterial populations are initially strongly depleted in the presence of parasites. During experimental evolution, total growth of bacteria was measured at each transfer. Independent populations are plotted as fine lines, and bold lines denote the mean in each treatment. Note the difference in y-axis scales due to incubation and media differences between the strong and weak phage conditions.

Isolate Characterization

After approximately 350 generations of experimental evolution, we isolated five evolved bacterial clones from the final timepoint in each replicate population. We then measured how parasite spatial distribution had altered the evolution of three traits: resistance to phage, dispersal in soft agar, and growth in liquid media.

Resistance to Phage

We measured the resistance of evolved bacteria to parasite infection (Fig 3). We found that parasite spatial distribution had a substantial effect on resistance evolution. In the weak phage condition, one local population and all global populations evolved increased levels of resistance. While in the strong phage condition, all populations in both the local and global treatments evolved increased levels of resistance.

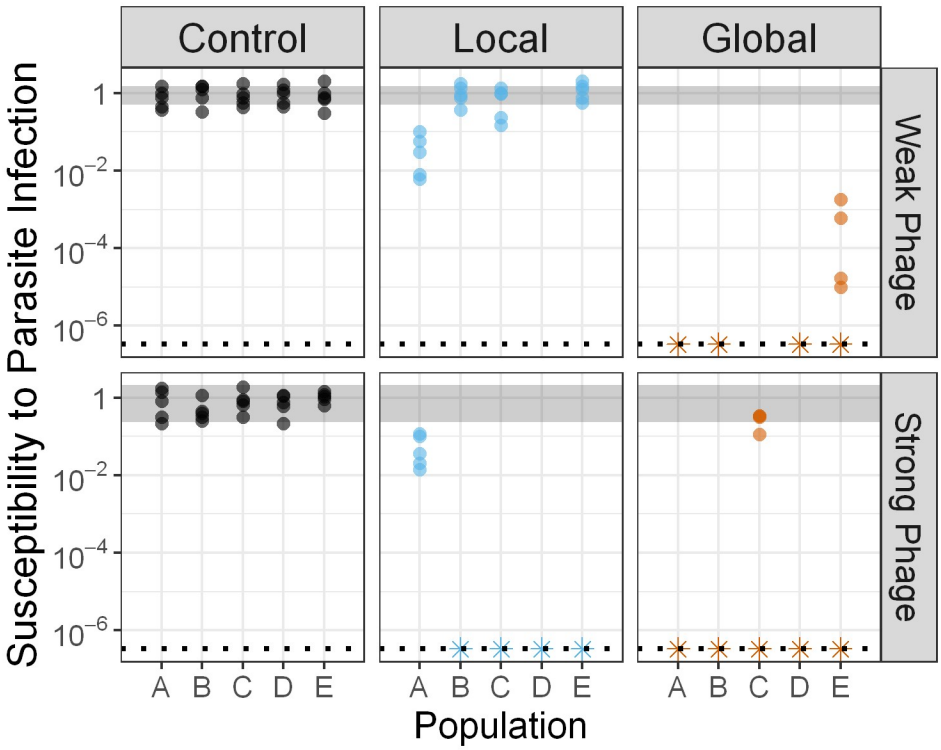

Figure 3. Bacteria evolve resistance in the presence of globally distributed or strongly growing parasites. Bacterial isolates from the final transfer of experimental evolution were assayed for their resistance to phage infection, relative to the ancestor. The gray region denotes the range of values observed for the ancestral bacteria. Isolates whose susceptibility fell below the limit of detection (dotted line) are plotted as a star.

Dispersal

We measured the dispersal rate of evolved bacteria in soft agar (Figs 4, S1). Evolved isolates tended to have increased dispersal relative to the ancestor, although this effect was non-significant (linear mixed-effects model of dispersal with random effects for population and batch and fixed effect for treatment, all contrasts with ancestor $p > 0.05$). However, parasite distribution did not drive increased evolution of dispersal rate (linear mixed effects model of delta dispersal with random effect for population and fixed effect for treatment, Kenward-Roger approximate F-test comparison to model with just population random effect $p = 0.78$ in weak phage conditions, $p = 0.03$ in strong phage conditions; Tukey-corrected pairwise contrasts in strong phage condition showed that control treatment evolved significantly higher dispersal than local or global treatments).

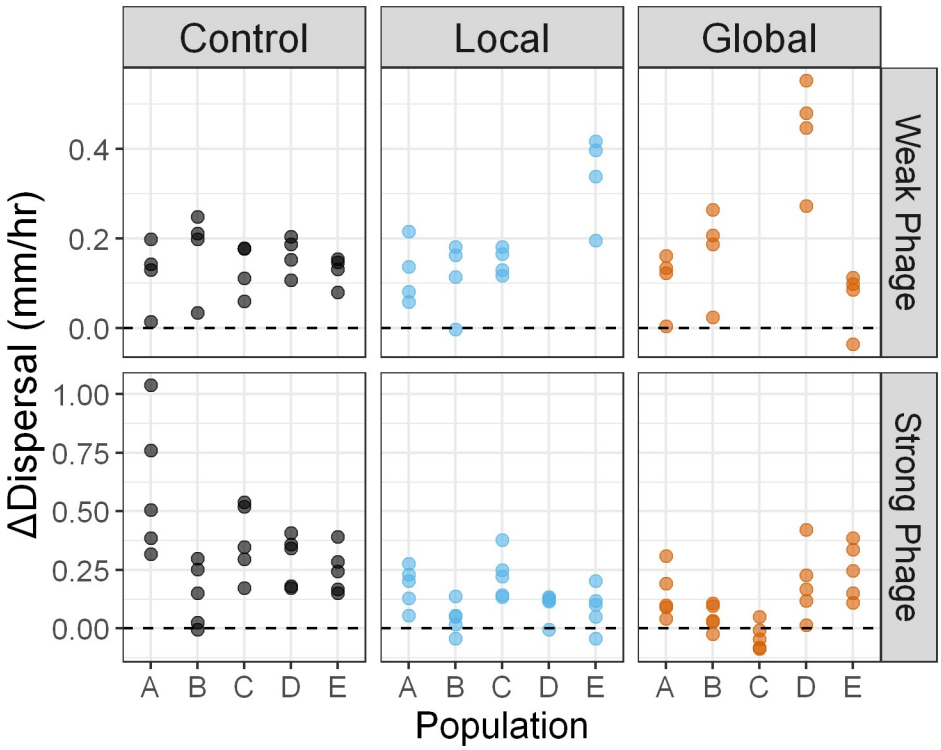

Figure 4. Bacteria evolved increased dispersal, regardless of parasite spatial distribution. Bacterial isolates from the final transfer of experimental evolution were assayed for their dispersal in soft agar in the absence of parasites. Dispersal rates are plotted as the difference from the ancestral rate (dashed line). Note the difference in y-axis scales due to incubation and media differences between the strong and weak phage conditions.

Growth in Liquid

We measured the growth rate of evolved bacteria in liquid media (Figs 5, S2). There was no significant effect of parasite distribution or evolved resistance on maximum per-capita growth rate (Table S2). This pattern also held true when isolates were grown in rich media containing elevated nutrient concentrations (Fig S2), and broadly for growth characteristics other than growth rate (Figs S3-S8).

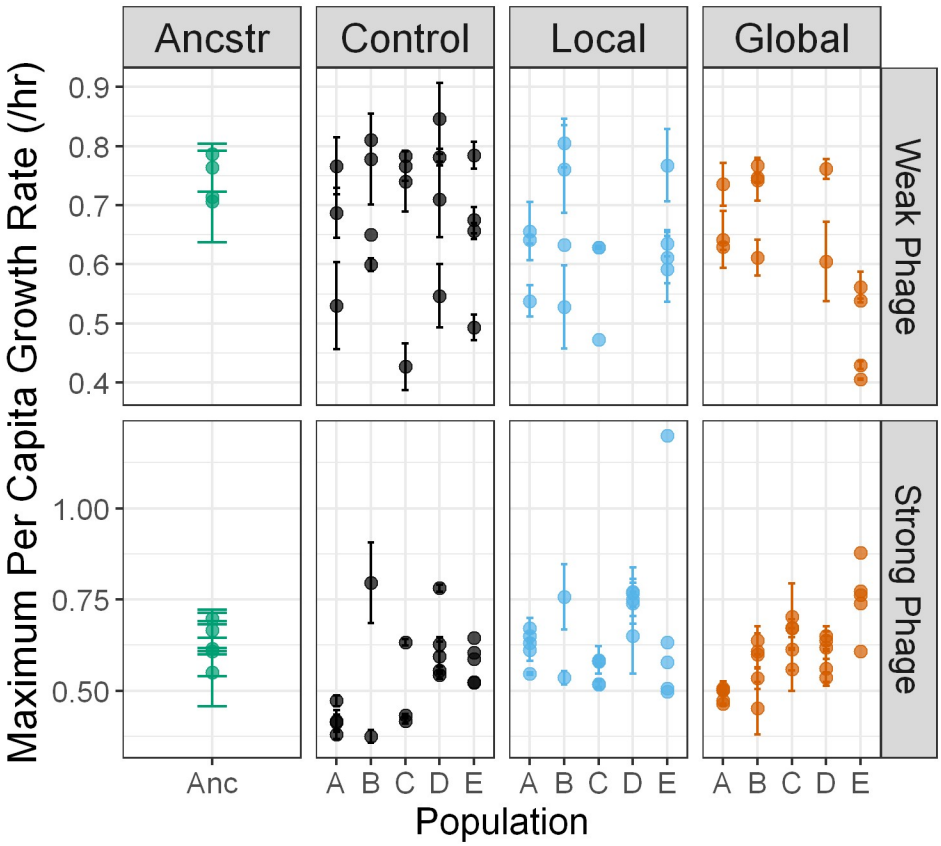

Figure 5. Evolved bacterial growth rates show no effects of parasite distribution. Bacterial isolates from the final transfer of experimental evolution were grown in liquid to quantify their maximum per-capita growth rate. Error bars denote the standard deviation between technical replicates for an isolate. Note the difference in y-axis scales due to incubation and media differences between the strong and weak phage conditions.

Mathematical Modeling

These results showing the evolution of resistance and not dispersal could be specific to any number of biological particularities of our model system. Unfortunately, establishing the generality of these findings *in vitro* is experimentally intractable (Lustenhouwer et al. 2023). Instead, we leveraged existing mathematical models of bacterial growth and dispersal to simulate bacterial evolution in the presence of different parasite spatial distributions across a wide range of bacterial trait values. Using *in silico* invasion experiments, we uncovered the fitness landscape between dispersal and resistance and how it shifted depending on parasite spatial distribution (Fig 6). As expected, in the absence of parasites, dispersal is selected for and resistance provides no benefits (Mattingly and Emonet 2022). Surprisingly, in the presence of parasites, regardless of their distribution, this pattern is exactly flipped: resistance is selected for, while dispersal provides no benefits. Moreover, this finding is robust to the form of the Global distribution (Fig S9), and is in sharp contrast to patterns observed with other traits, like growth

rate or yield, where parasite presence strengthens selection for resistance without weakening selection for the alternative trait (Figs S10-S12).

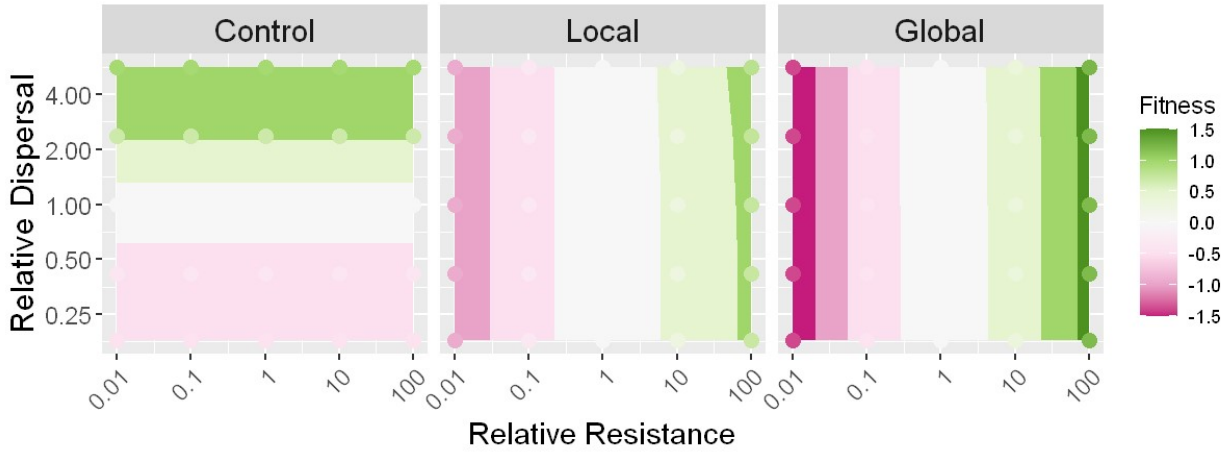

Figure 6. Parasite presence selects for host resistance and eliminates selection for host dispersal. *In silico* invasion experiments were carried out with a bacterial mutant that varied in its traits relative to the resident bacterial population, both competing in the presence of one of three different initial parasite spatial distributions. Each point is the result of a simulated invasion, colored by invader fitness = $\log_{10}$(final invader frequency/final resident frequency). Contours are interpolated for visualization.

Discussion

Here we directly tested whether bacterial dispersal can evolve to avoid parasites. In our *in vitro* experimental evolution, we found that bacterial hosts adapted to parasites not by the evolution of dispersal, but via the evolution of resistance (Figs 3-4). Our *in silico* simulations expanded the generality of our empirical conclusions, showing that parasite presence eliminates selection for greater dispersal (Fig 6).

Our findings build on past studies of bacterial dispersal in semi-solid environments in the presence of parasitic phages, and in particular two manuscripts which highlighted the potential for dispersal evolution. Li et al studied the ecological dynamics of *Salmonella enterica* as it dispersed in soft agar in the presence of χ phages (Li et al. 2020). Their experiments showed spatial co-propagation when phages and bacteria had similar dispersal speeds. Based on those results, they predicted that over longer evolutionary time scales, bacteria and phages could be in a coevolutionary arms race to evolve faster dispersal. Second, Taylor & Buckling studied the competitive benefits of *Pseudomonas aeruginosa* motility in the presence of different spatial distributions of phage PhiKZ (Taylor and Buckling 2013). They found that motility was beneficial in the presence of phages regardless of the spatial distribution of those phages. Based on those results, they argued that phages have the potential to select for bacterial dispersal. These two ecological studies made evolutionary predictions. However, those predictions did not pan out in our direct evolutionary tests, where we find that phages do not select for bacterial dispersal (Figs 4, 6).

In contrast, our findings generally align with the work of Ping et al, who studied the ecology and evolution of *E. coli* and phage P1 as they disperse in soft agar from a shared inoculation site (Ping et al. 2020). In their experiments, and associated mathematical modeling, they found that bacteria are selected for phage resistance when they do not disperse fast enough to avoid diffusing phages. However, they did not directly test whether phages would alter selection on dispersal, and their modeling assumed a constant cost of phage resistance. Our findings directly showed that phages do *not* select for bacterial dispersal (Figs 4, 6), and showed that resistance is favored over avoidance across the whole fitness landscape (Fig 6).

Our results also generally follow previously reported trends on the evolution of bacteria under selection by phages. At the beginning of the evolution experiment, we observed depletion of bacterial populations in treatments containing phages, before populations recovered in subsequent passages (Fig 2). Such dynamics are common in phage-bacteria experiments where bacteria are initially susceptible (Koskella et al. 2011). At the end of the experiment, we found that populations in our global phage treatment evolved resistance regardless of the strength of phage growth (Fig 3). This is similar to past work where more homogenous environments accelerated the coevolution of bacterial resistance with phages (Brockhurst et al. 2003). Additionally, we found that evolved populations in our local phage treatment maintained phage susceptibility that could enable coexistence of bacteria and phages (Fig 3), consistent with past work that spatial structure and heterogeneity increases host-parasite coexistence (Brockhurst et al. 2006; Tamar and Kishony 2022).

We were surprised to find the maintenance of intra-population variation in resistance, especially in bacteria from the global parasites treatment. In particular, two populations contain isolates whose resistance differs by many orders of magnitude (Fig 3). Not only is this surprising given the strong selection for resistance generally observed in the global treatment, but also because our experimental design imposed severe bottlenecks on the effective population size that should tend to purge intrapopulation diversity. Although each transfer population was ~10^6 individuals, bacteria dispersing in spatially structured environments tend to neutrally self-assort in space (Gralka et al. 2016). Because of this, bacteria in a sample taken from a single random point on the colony's edge will be much more closely related to each other than a random sample of bacteria from the entire colony would be. Several mechanisms could explain this result, including a lack of neutral spatial self-assortment in our system or plasticity such that resistance differs between the evolution and resistance assay conditions. Further work is needed to resolve an explanation.

Previous work has also commonly found relationships between evolved bacterial traits, something we unexpectedly failed to consistently find in our data (Figs S7, S8). For instance, past work with *P. fluorescens* and Phi2 has documented a tradeoff between competitive ability and phage resistance (Brockhurst et al. 2004), and that coevolution with phages can constrain adaptation to the abiotic environment (Scanlan et al. 2015). We found neither of these patterns in our data. In related work, Koskella et al found that pressure to evolve phage resistance in *Pseudomonas* species can constrain the evolution of increased growth in soft agar (Koskella et al. 2011), something we did not find in our experiments. However, they also reported that bacterial motility had no negative relationship with resistance to phage nor with growth rate, consistent with our findings. Finally, (Fraebel et al. 2017) have previously reported that dispersal in soft agar in *Escherichia coli* is constrained by a tradeoff between growth rate and run speed during swimming. This may imply that increased dispersal should trade-off with growth rate. However, we did not observe this pattern in our data, suggesting that the increased

dispersal we observed arose via a less costly mechanism like modulating tumble bias (Wolfe and Berg 1989; Koster et al. 2012; Ni et al. 2017).

Bacteria have abundant strategies to resist phage infection (Hampton et al. 2020), including the capability to activate defenses when they detect infections in nearby neighbors (de Mattos et al. 2022), as well as complex abilities to sense and physically navigate their environment (Keegstra et al. 2022; Wadhwa and Berg 2022). Despite the widespread existence of host avoidance of parasites in mobile eukaryotes (Gibson and Amoroso 2022), our experiments and theory suggest that bacterial avoidance of parasites may only rarely, if ever, be selected for.

References

Bache, S. M., and H. Wickham. 2022. magrittr: A Forward-Pipe Operator for R.
Baines, C. B., S. Diab, and S. J. McCauley. 2020. Parasitism Risk and Infection Alter Host Dispersal. The American Naturalist 196:119–131.
Baranyi, J., and T. A. Roberts. 1994. A dynamic approach to predicting bacterial growth in food. International Journal of Food Microbiology 23:277–294.
Bar-On, Y. M., R. Phillips, and R. Milo. 2018. The biomass distribution on Earth. Proceedings of the National Academy of Sciences 115:6506–6511.
Bates, D., M. Mächler, B. Bolker, and S. Walker. 2015. Fitting Linear Mixed-Effects Models Using lme4. Journal of Statistical Software 67:1–48.
Blazanin, M. 2023. gcplyr: an R package for microbial growth curve data analysis. bioRxiv.
Boulinier, T., K. D. McCoy, and G. Sorci. 2001. Dispersal and parasitism. Page 480 *in* J. Clobert, E. Danchin, A. A. Dhondt, and J. D. Nichols, eds. Dispersal (1st ed.). Oxford University Press.
Brand, T. van den. 2022. ggh4x: Hacks for "ggplot2."
Brockhurst, M. A., A. Buckling, and P. B. Rainey. 2006. Spatial heterogeneity and the stability of host-parasite coexistence. Journal of Evolutionary Biology 19:374–379.
Brockhurst, M. A., A. D. Morgan, A. Fenton, and A. Buckling. 2007. Experimental coevolution with bacteria and phage. The Pseudomonas fluorescens—Φ2 model system. Infection, Genetics and Evolution 7:547–552.
Brockhurst, M. A., A. D. Morgan, P. B. Rainey, and A. Buckling. 2003. Population mixing accelerates coevolution. Ecology Letters 6:975–979.
Brockhurst, M. A., P. B. Rainey, and A. Buckling. 2004. The effect of spatial heterogeneity and parasites on the evolution of host diversity. Proceedings of the Royal Society B 271:107–11.
Brophy, T., and L. T. Luong. 2021. The influence of infection status and parasitism risk on host dispersal and susceptibility to infection in *Drosophila nigrospiracula*. Parasitology 1–6.
Cremer, J., T. Honda, Y. Tang, J. Wong-Ng, M. Vergassola, and T. Hwa. 2019. Chemotaxis as a navigation strategy to boost range expansion. Nature 575:658–663.
Croze, O. A., G. P. Ferguson, M. E. Cates, and W. C. K. Poon. 2011. Migration of Chemotactic Bacteria in Soft Agar: Role of Gel Concentration. Biophysical Journal 101:525–534.
de Mattos, C. D., A. A. Nemudryi, D. Faith, D. C. Bublitz, L. Hammond, M. A. Kinnersley, C. M. Schwartzkopf, et al. 2022. *Bacterial threat assessment of bacteriophage infection is mediated by intracellular polyamine accumulation and Gac/Rsm signaling* (preprint). Microbiology.

Finlay, B. J., S. C. Maberly, and J. I. Cooper. 1997. Microbial diversity and ecosystem function. Oikos 209–213.
Fraebel, D. T., H. Mickalide, D. Schnitkey, J. Merritt, E. Kuhlman, and S. Kuehn. 2017. Environment determines evolutionary trajectory in a constrained phenotypic space. eLife 6:1–26.
Gibson, A. K., and C. R. Amoroso. 2022. Evolution and Ecology of Parasite Avoidance. Annual Review of Ecology, Evolution, and Systematics 53:annurev-ecolsys-102220-020636.
Gralka, M., F. Stiewe, F. Farrell, W. Möbius, B. Waclaw, and O. Hallatschek. 2016. Allele surfing promotes microbial adaptation from standing variation. Ecology Letters 889–898.
Halekoh, U., and S. Højsgaard. 2014. A Kenward-Roger Approximation and Parametric Bootstrap Methods for Tests in Linear Mixed Models – The R Package pbkrtest. Journal of Statistical Software 59:1–30.
Hall, M. D., G. Bento, and D. Ebert. 2017. The Evolutionary Consequences of Stepwise Infection Processes. Trends in Ecology & Evolution 32:612–623.
Hampton, H. G., B. N. J. Watson, and P. C. Fineran. 2020. The arms race between bacteria and their phage foes. Nature 577:327–336.
Harshey, R. M. 2003. Bacterial Motility on a Surface: Many Ways to a Common Goal. Annual Review of Microbiology 57:249–273.
Hendrix, R. W., G. F. Hatfull, M. E. Ford, M. C. M. Smith, and R. N. Burns. 1999. Evolutionary relationships among diverse bacteriophages and prophages: all the world's a phage. Proceedings of the National Academy of Sciences 96:2192–2197.
Keegstra, J. M., F. Carrara, and R. Stocker. 2022. The ecological roles of bacterial chemotaxis. Nature Reviews Microbiology 20:491–504.
Keller, E. F., and L. A. Segel. 1970. Initiation of slime mold aggregation viewed as an instability. Journal of theoretical biology 26:399–415.
Kohler, T., L. K. Curty, F. Barja, C. Van Delden, and J. C. Pechere. 2000. Swarming of Pseudomonas aeruginosa is dependent on cell-to-cell signaling and requires flagella and pili. Journal of Bacteriology 182:5990–5996.
Kortright, K. E., B. K. Chan, J. L. Koff, and P. E. Turner. 2019. Phage Therapy: A Renewed Approach to Combat Antibiotic-Resistant Bacteria. Cell Host and Microbe 25:219–232.
Koskella, B., T. B. Taylor, J. Bates, and A. Buckling. 2011. Using experimental evolution to explore natural patterns between bacterial motility and resistance to bacteriophages. The ISME Journal 5:1809–1817.
Koster, D. A., A. Mayo, A. Bren, and U. Alon. 2012. Surface growth of a motile bacterial population resembles growth in a chemostat. Journal of Molecular Biology 424:180–191.
Li, X., F. Gonzalez, N. Esteves, B. E. Scharf, and J. Chen. 2020. Formation of phage lysis patterns and implications on co-propagation of phages and motile host bacteria. (B. Althouse, ed.)PLOS Computational Biology 16:e1007236.
Lustenhouwer, N., F. Moerman, F. Altermatt, R. D. Bassar, G. Bocedi, D. Bonte, S. Dey, et al. 2023. Experimental evolution of dispersal: Unifying theory, experiments and natural systems. Journal of Animal Ecology.
Mattingly, H. H., and T. Emonet. 2022. Collective behavior and nongenetic inheritance allow bacterial populations to adapt to changing environments. Proceedings of the National Academy of Sciences 119:e2117377119.
Millman, A., A. Bernheim, A. Stokar-Avihail, T. Fedorenko, M. Voichek, A. Leavitt, Y. Oppenheimer-Shaanan, et al. 2020. Bacterial Retrons Function In Anti-Phage Defense. Cell 183:1551-1561.e12.

Millman, A., S. Melamed, A. Leavitt, S. Doron, A. Bernheim, J. Hör, J. Garb, et al. 2022. An expanded arsenal of immune systems that protect bacteria from phages. Cell Host & Microbe 30:1556-1569.e5.
Mushegian, A. R. 2020. Are there 10^31 virus particles on Earth, or more, or less? Journal of Bacteriology 202:e00052-20.
Ni, B., B. Ghosh, F. S. Paldy, R. Colin, T. Heimerl, and V. Sourjik. 2017. Evolutionary remodeling of bacterial motility checkpoint control. Cell reports 18:866–877.
Okabe, M., and K. Ito. 2008. Color universal design (cud)-how to make figures and presentations that are friendly to colorblind people.
Padfield, D., M. Castledine, and A. Buckling. 2019. Temperature-dependent changes to host-parasite interactions alter the thermal performance of a bacterial host. The ISME Journal 1–23.
Patlak, C. S. 1953. Random walk with persistence and external bias. The bulletin of mathematical biophysics 15:311–338.
Ping, D., T. Wang, D. T. Fraebel, S. Maslov, K. Sneppen, and S. Kuehn. 2020. Hitchhiking, collapse, and contingency in phage infections of migrating bacterial populations. The ISME Journal 14:2007–2018.
R Core Team. 2022. R: A Language and Environment for Statistical Computing. R Foundation for Statistical Computing, Vienna, Austria.
Ram, Y., E. Dellus-Gur, M. Bibi, K. Karkare, U. Obolski, M. W. Feldman, T. F. Cooper, et al. 2019. Predicting microbial growth in a mixed culture from growth curve data. Proceedings of the National Academy of Sciences 201902217.
Sampedro, I., R. E. Parales, T. Krell, and J. E. Hill. 2015. Pseudomonas chemotaxis. FEMS Microbiology Reviews 39:17–46.
Scanlan, P. D., and A. Buckling. 2012. Co-evolution with lytic phage selects for the mucoid phenotype of Pseudomonas fluorescens SBW25. The ISME Journal 6:1148–58.
Scanlan, P. D., A. R. Hall, G. Blackshields, V.-P. Friman, M. R. Davis, J. B. Goldberg, and A. Buckling. 2015. Coevolution with bacteriophages drives genome-wide host evolution and constrains the acquisition of abiotic-beneficial mutations. Molecular Biology and Evolution 32:1425–35.
Schindelin, J., I. Arganda-Carreras, E. Frise, V. Kaynig, M. Longair, T. Pietzsch, S. Preibisch, et al. 2012. Fiji: an open-source platform for biological-image analysis. Nature Methods 9:676–682.
Sloggett, J. J., and W. W. Weisser. 2002. Parasitoids induce production of the dispersal morph of the pea aphid, Acyrthosiphon pisum. Oikos 98:323–333.
Slowikowski, K. 2022. ggrepel: Automatically Position Non-Overlapping Text Labels with "ggplot2."
Tamar, E. S., and R. Kishony. 2022. Multistep diversification in spatiotemporal bacterial-phage coevolution. Nature Communications 13:7971.
Taylor, T. B., and A. Buckling. 2013. Bacterial motility confers fitness advantage in the presence of phages. Journal of Evolutionary Biology 26:2154–2160.
Vogwill, T., A. Fenton, and M. A. Brockhurst. 2008. The impact of parasite dispersal on antagonistic host-parasite coevolution. Journal of Evolutionary Biology 21:1252–1258.
Wadhwa, N., and H. C. Berg. 2022. Bacterial motility: machinery and mechanisms. Nature Reviews Microbiology 20:161–173.
Weisser, W. W. 2001. The effects of predation on dispersal. Page 480 *in* J. Clobert, E. Danchin, A. A. Dhondt, and J. D. Nichols, eds. Dispersal (1st ed.). Oxford University Press.

Weitz, J., and S. Wilhelm. 2012. Ocean viruses and their effects on microbial communities and biogeochemical cycles. F1000 Biology Reports 8:2–9.
Whitman, W. B., D. C. Coleman, and W. J. Wiebe. 1998. Prokaryotes: The unseen majority. Proceedings of the National Academy of Sciences 95:6578–6583.
Wickham, H. 2007. Reshaping data with the reshape package. Journal of Statistical Software 21.
———. 2016. ggplot2: Elegant Graphics for Data Analysis. Springer-Verlag New York.
Wickham, H., R. François, L. Henry, and K. Müller. 2023*a*. dplyr: A Grammar of Data Manipulation.
Wickham, H., and L. Henry. 2023. purrr: Functional Programming Tools.
Wickham, H., D. Vaughan, and M. Girlich. 2023*b*. tidyr: Tidy Messy Data.
Wilke, C. O. 2020. cowplot: Streamlined Plot Theme and Plot Annotations for "ggplot2."
Wilke, C. O., and B. M. Wiernik. 2022. ggtext: Improved Text Rendering Support for "ggplot2."
Wolfe, A. J., and H. C. Berg. 1989. Migration of bacteria in semisolid agar. Proceedings of the National Academy of Sciences 86:6973–6977.
Wommack, K. E., and R. R. Colwell. 2000. Virioplankton: viruses in aquatic ecosystems. Microbiology and Molecular Biology Reviews 64:69–114.
Zilio, G., L. S. Nørgaard, G. Petrucci, N. Zeballos, C. Gougat-Barbera, E. A. Fronhofer, and O. Kaltz. 2021. Parasitism and host dispersal plasticity in an aquatic model system. Journal of Evolutionary Biology 34:1316–1325.

Supplementary Materials

Repeated passages

Table S1. Repeated Passages Due to Sampling. During experimental evolution seven transfers failed to show growth in at least one treatment after 24 hours, likely due to sampling effects of the low-density cell front. In these instances, a new set of plates was re-inoculated from the previous plates, which had been stored at 4C.

Condition	Replicate Population	Transfer
Weak phage	A	2
Weak phage	B	2
Weak phage	B	6
Weak phage	B	7
Strong phage	C	1
Strong phage	D	1
Strong phage	D	2

Evolved dispersal

We measured the dispersal rate of evolved bacteria in soft agar. To reduce batch effects, in the main text we report the difference in soft agar dispersal of each evolved isolate from a same-batch ancestral plate (Fig 4). Here, we report the unnormalized soft agar dispersal values (Fig S1).

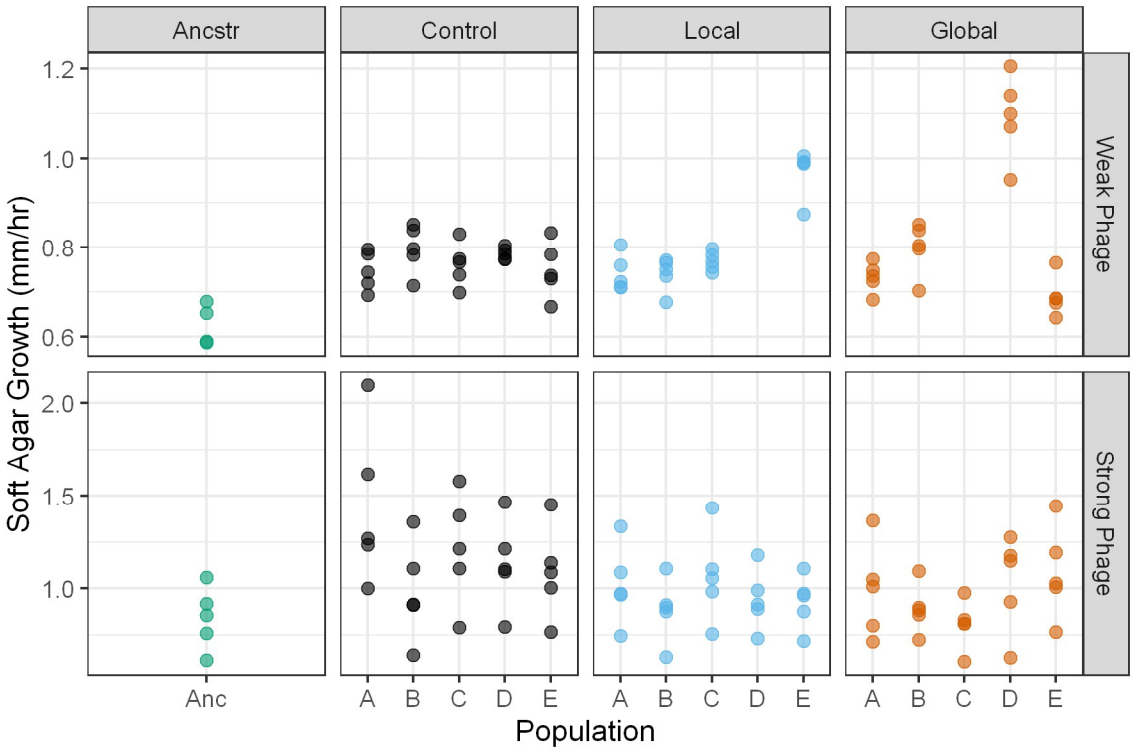

Figure S1. Bacteria evolved increased dispersal, regardless of parasite spatial distribution. Bacterial isolates from the final transfer of experimental evolution were assayed for their dispersal in soft agar in the absence of parasites. Note the difference in y-axis scales due to incubation and media differences between the strong and weak phage conditions.

Evolved growth

During experimental evolution, bacteria may have adapted their growth characteristics and life history traits to the different treatments. Alternatively, these traits may have evolved following trade-offs with other traits that were under selection, like resistance to phages or dispersal in soft agar. To measure growth characteristics, we collected growth curves of evolved isolates from the final timepoint in liquid media. Each isolate was grown in their experimental evolution environment ("original"), as well as an environment with all nutrients doubled in concentration ("rich"). This rich media was included to possibly reveal cases when bacteria had evolved growth costs due to trade-offs with dispersal or resistance that had then been ameliorated by compensatory mutations. By doubling the nutrients, we hypothesized this may reveal any costs of evolution hidden by compensatory mutations.

Growth curves were computationally characterized, with computational findings manually validated, as described in the main text. In particular, we identified the following traits:

- Maximum per-capita growth rate (r)
- Lag time (time when maximum per-capita growth first exceeded 0.5/hr, or 0.4/hr when 0.5 was never reached)
- Time when a diauxic shift occurred, if any (k_t)
- Density when a diauxic shift occurred, if any (k)
- Deceleration parameter as bacterial density approaches diauxic shift (v)

Maximum per-capita growth rate in the original media was reported in the main text (Fig 5). Here, we report all these traits across both medias.

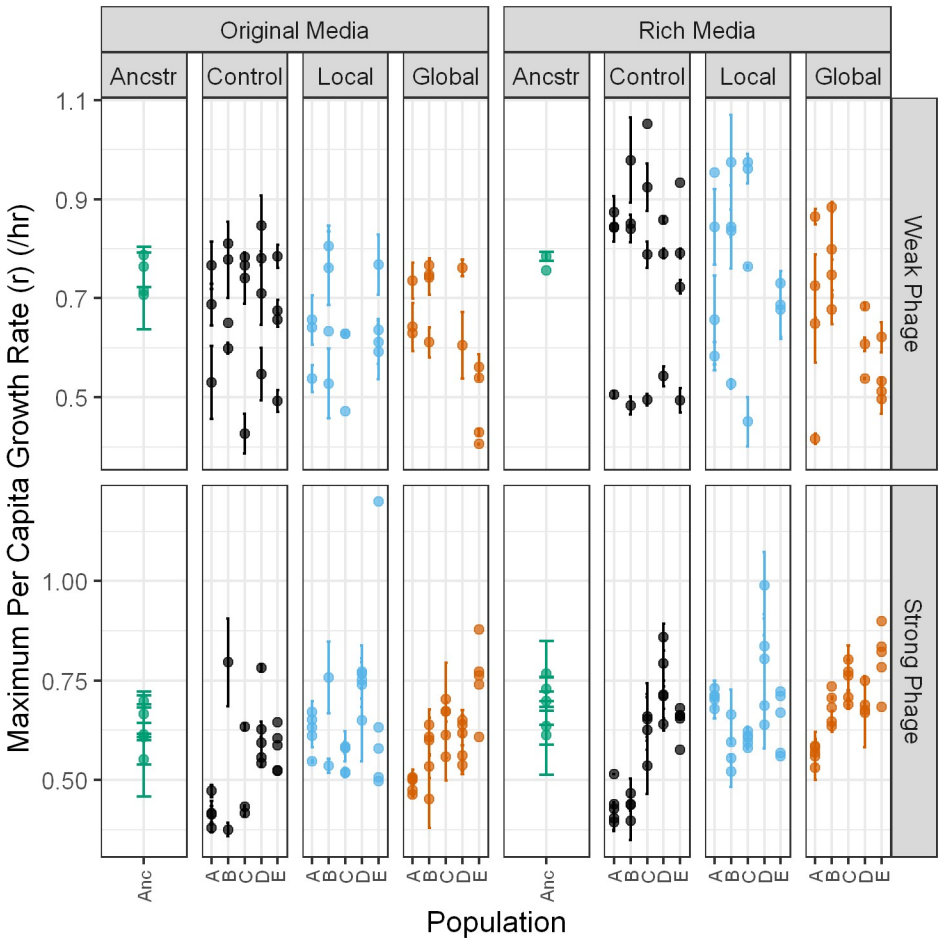

Figure S2. Evolution of maximum per capita growth rate. Growth curves of ancestral and evolved bacterial isolates were collected in liquid media containing the same (original) or double (rich) the nutrients as experienced during experimental evolution. Each point represents the mean of two replicate wells containing the same isolate, with isolates from the same population stacked vertically, and error bars denoting the standard deviation between replicate wells. Note the difference in y-axis scales due to incubation and media differences between the strong and weak phage conditions.

Table S2. Statistical tests for differences in maximum per-capita growth rate. Mixed effects modeling of maximum per-capita growth rate was carried out using lmer. As a null model, we included random effects for the population and for the batch date. We then compared this null model to models with fixed effects with a Kenward-Roger approximate F-test. We included a fixed effect for treatment [ancestor, control, local, or global], a fixed effect for resistance [none, partial (EOP above detection limit but below 0.1), or complete (EOP below detection limit)], or both. No tests were significant, indicating that neither treatment nor resistance were significantly associated with evolved maximum per-capita growth rate in either condition or media.

Condition	Media	Fixed Effects	Approximate F-Statistic	p-value
Weak phage	Original	Treatment	1.57	0.26
Weak phage	Rich	Treatment	2.64	0.09
Weak phage	Original	Resistance	2.49	0.11
Weak phage	Rich	Resistance	2.56	0.11
Weak phage	Original	Treatment + Resistance	2.96	0.07
Weak phage	Rich	Treatment + Resistance	1.30	0.33
Strong phage	Original	Treatment	2.03	0.16
Strong phage	Rich	Treatment	1.25	0.34
Strong phage	Original	Resistance	0.80	0.46
Strong phage	Rich	Resistance	0.35	0.71
Strong phage	Original	Treatment + Resistance	1.24	0.34
Strong phage	Rich	Treatment + Resistance	0.72	0.62

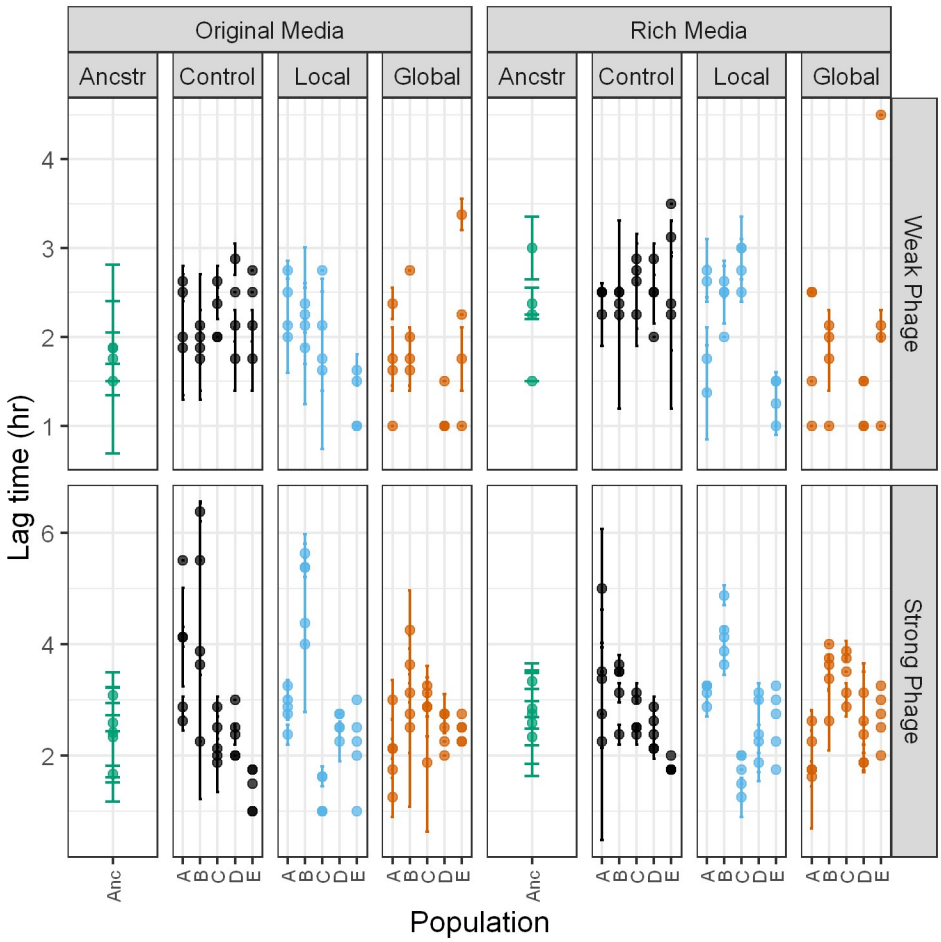

Figure S3. Evolution of lag time. Growth curves of ancestral and evolved bacterial isolates were collected in liquid media containing the same (original) or double (rich) the nutrients as experienced during experimental evolution. Each point represents the mean of two replicate wells containing the same isolate, with isolates from the same population stacked vertically, and error bars denoting the standard deviation between replicate wells. Note the difference in y-axis scales due to incubation and media differences between the strong and weak phage conditions.

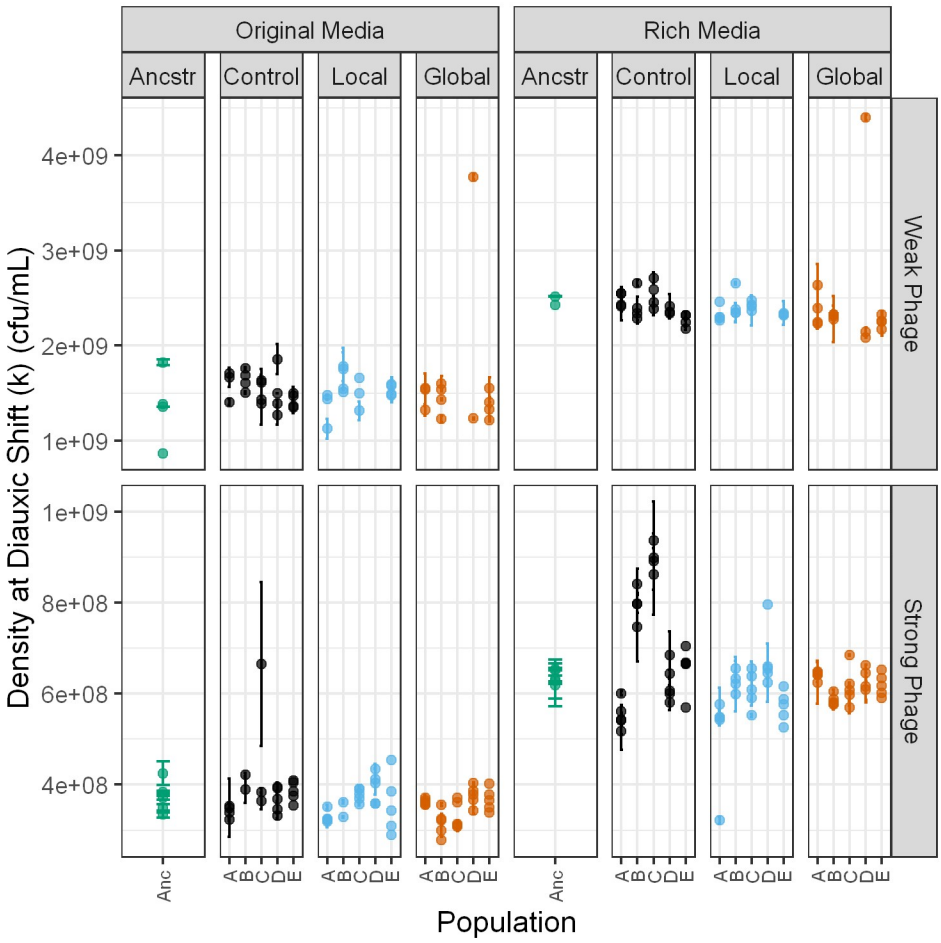

Figure S4. Evolution of diauxic shift density. Growth curves of ancestral and evolved bacterial isolates were collected in liquid media containing the same (original) or double (rich) the nutrients as experienced during experimental evolution. Each point represents the mean of two replicate wells containing the same isolate, with isolates from the same population stacked vertically, and error bars denoting the standard deviation between replicate wells. Points that are outliers with high diauxic shift densities were curves where the bacteria did not undergo a computationally identifiable diauxic shift. Note the difference in y-axis scales due to incubation and media differences between the strong and weak phage conditions.

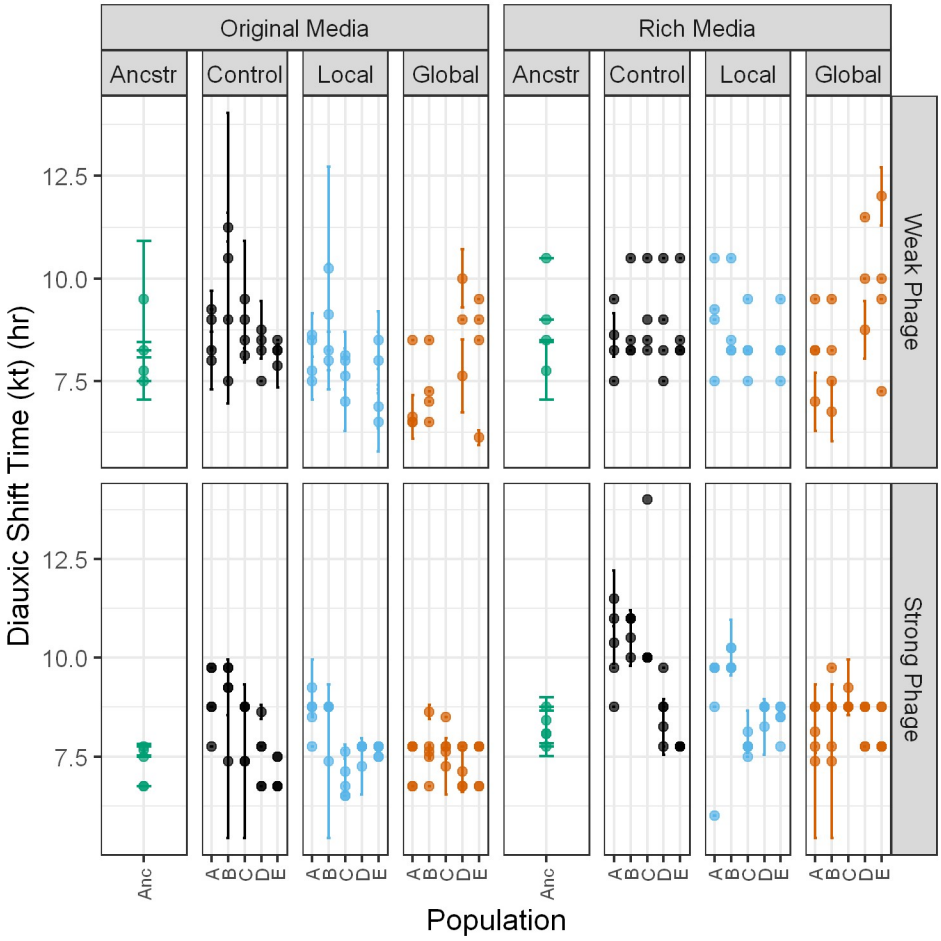

Figure S5. Evolution of diauxic shift timing. Growth curves of ancestral and evolved bacterial isolates were collected in liquid media containing the same (original) or double (rich) the nutrients as experienced during experimental evolution. Each point represents the mean of two replicate wells containing the same isolate, with isolates from the same population stacked vertically, and error bars denoting the standard deviation between replicate wells. Note the difference in y-axis scales due to incubation and media differences between the strong and weak phage conditions.

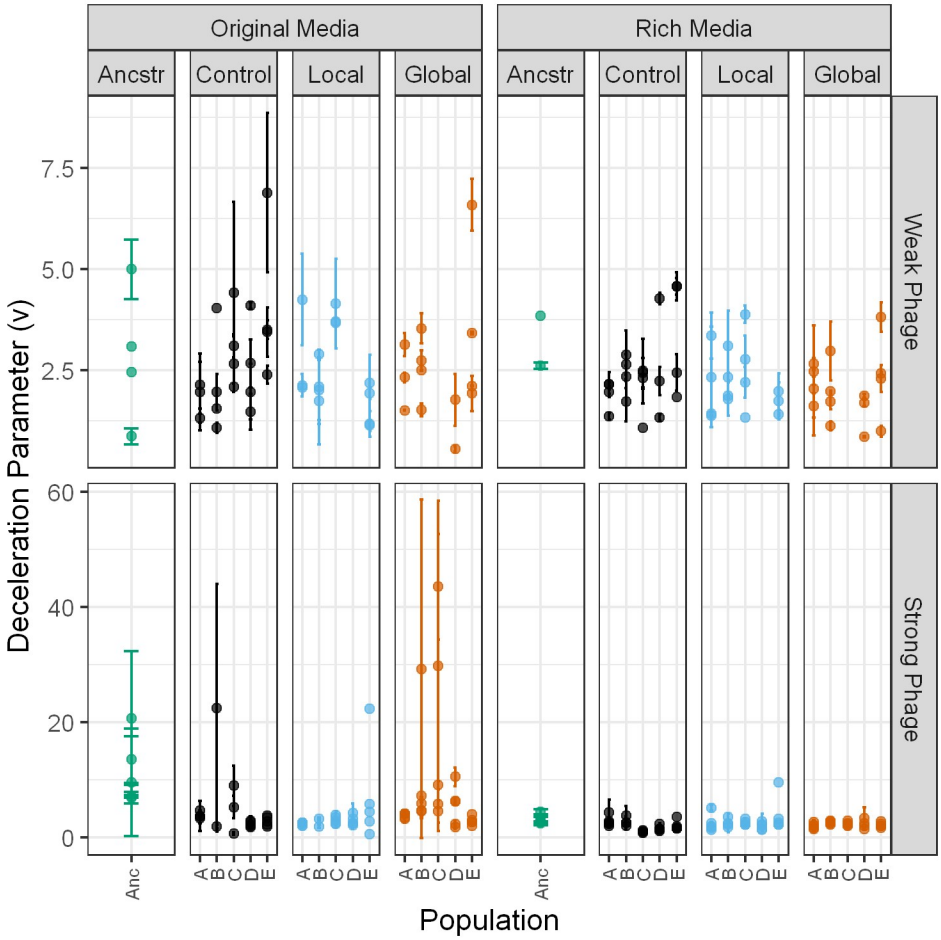

Figure S6. Evolution of deceleration parameter. Growth curves of ancestral and evolved bacterial isolates were collected in liquid media containing the same (original) or double (rich) the nutrients as experienced during experimental evolution. Each point represents the mean of two replicate wells containing the same isolate, with isolates from the same population stacked vertically, and error bars denoting the standard deviation between replicate wells. Note the difference in y-axis scales due to incubation and media differences between the strong and weak phage conditions.

Relationships among evolved traits

To identify relationships among evolved traits in bacterial isolates, including dispersal, resistance to phages, and growth characteristics, we merged all three datasets characterizing the ancestral and evolved isolates. We then excluded any isolates with missing data. We carried out checks for univariate normalcy of all variables, and transformed some variables for improved normalcy: resistance was -$\log_{10}$(Efficiency of Plaquing), and diauxic shift density (k) was $\log_{10}$(k). Data from the weak phage condition-evolved bacteria was multivariate normal, while data from the strong phage condition-evolved bacteria was not multivariate normal. Data was scaled and centered and principal component analyses were run.

Generally, multivariate analyses reveal that growth traits were highly correlated between the original and rich medias within a condition (weak phage or strong phage) (Fig S7). In contrast, growth traits tended to have inconsistent relationships across the two conditions. We observe that global treatment isolates have most diverged from the ancestor in weak phage conditions, while control treatment populations have most diverged from the ancestor in strong phage conditions (Fig S8).

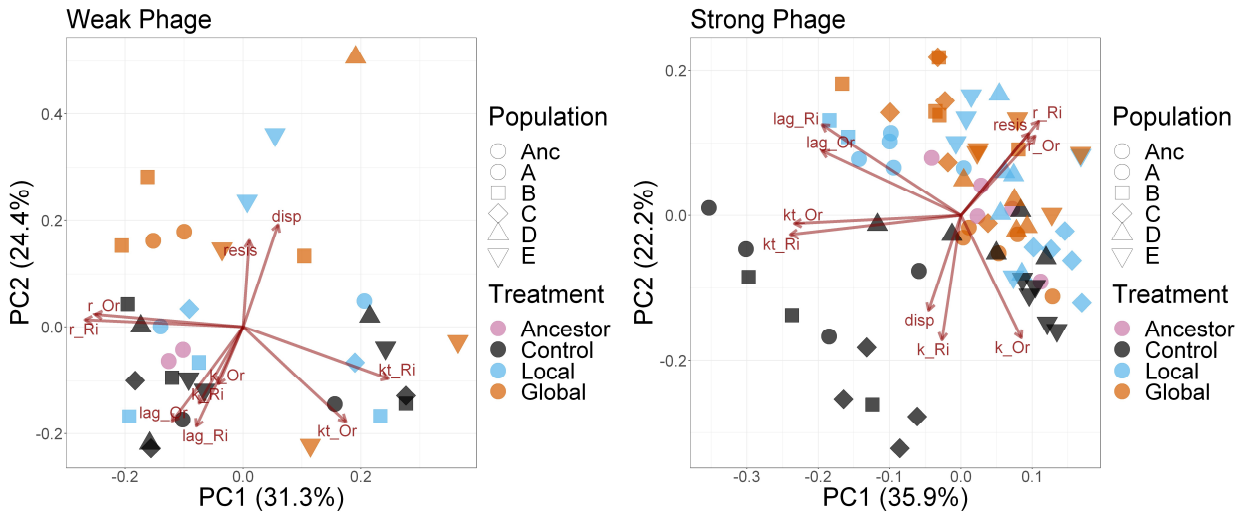

Figure S7. Multivariate evolution of bacterial traits. Data from growth curves, dispersal, and resistance assays were combined, normalized, and principal component analyses were run. Shown is a correlation biplot for each of the two conditions. Each point corresponds to a single isolate. Resis is -$\log_{10}$(Efficiency of Plaquing) and disp is dispersal rate. Growth characteristics of lag time (lag), maximum per-capita growth rate (r), the density at diauxic shift (k), and the time of diauxic shift (kt) were measured in media containing the original concentration of nutrients as used in experimental evolution (Or), and rich media containing double the nutrient concentration (Ri). Note that there are incubation and media differences between the strong and weak phage conditions.

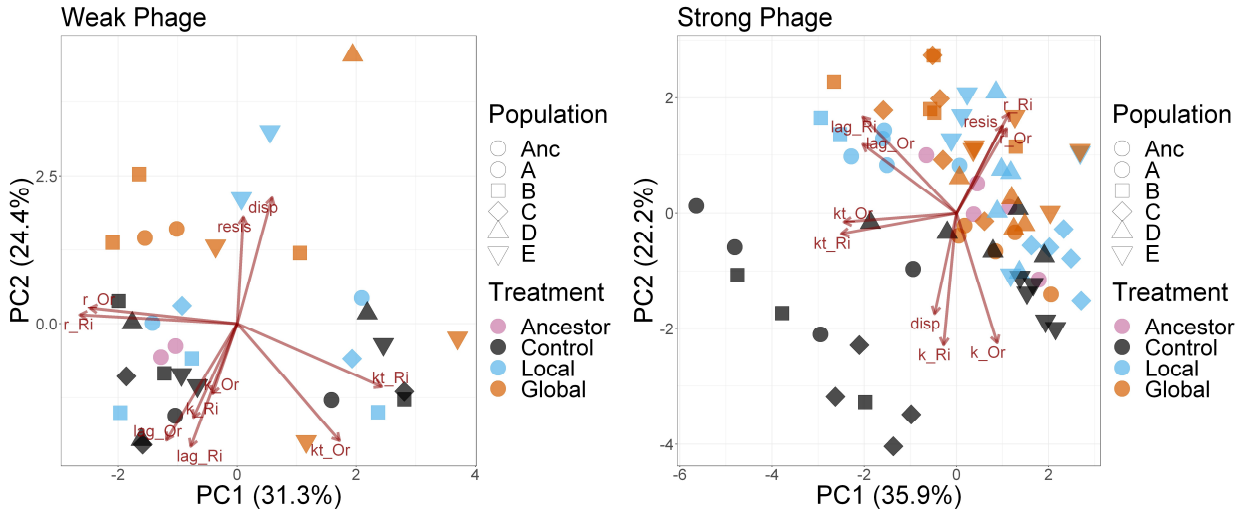

Figure S8. Multivariate evolution of bacterial traits. Data from growth curves, dispersal, and resistance assays were combined, normalized, and principal component analyses were run. Shown is a distance biplot for each of the two conditions. Each point corresponds to a single isolate. Resis is $-\log_{10}$(Efficiency of Plaquing) and disp is dispersal rate. Growth characteristics of lag time (lag), maximum per-capita growth rate (r), the density at diauxic shift (k), and the time of diauxic shift (kt) were measured in media containing the original concentration of nutrients as used in experimental evolution (Or), and rich media containing double the nutrient concentration (Ri). Note that there are incubation and media differences between the strong and weak phage conditions.

Simulation results

As described in the main text, we leveraged existing mathematical models of bacterial growth and dispersal to simulate bacterial evolution in the presence of different parasite spatial distributions across a wide range of bacterial trait values. Using *in silico* invasion experiments, we uncovered the fitness landscape between resistance and other bacterial traits. In the main text we report the fitness landscape between resistance and dispersal with three initial parasite distributions: none, gaussian-distributed (local), and uniformly-distributed (global) (Fig 6). Here, we include an additional "global" parasite distribution that uses a wider gaussian distribution, controlling for possible effects of gaussian vs uniform initial parasite distributions (Fig S9). We also report fitness landscapes between resistance and growth rate (Fig S10), yield (Fig S11), or attractant consumption (Fig S12).

These fitness landscapes reveal that, in the absence of parasites, increased dispersal, growth rate, and yield are adaptive, while (as expected) resistance is neutral. In the presence of parasites, resistance becomes adaptive. In landscapes of resistance with growth rate and yield, this has the effect of making both resistance and the other trait adaptive. However, strikingly, in the landscape of resistance and dispersal, dispersal loses its fitness benefits, suggesting that the unique dynamics of resistance and dispersal evolution eliminate the benefits of dispersal in the presence of parasites. These patterns only become more pronounced when comparing local to global to global (gaussian) initial parasite distributions.

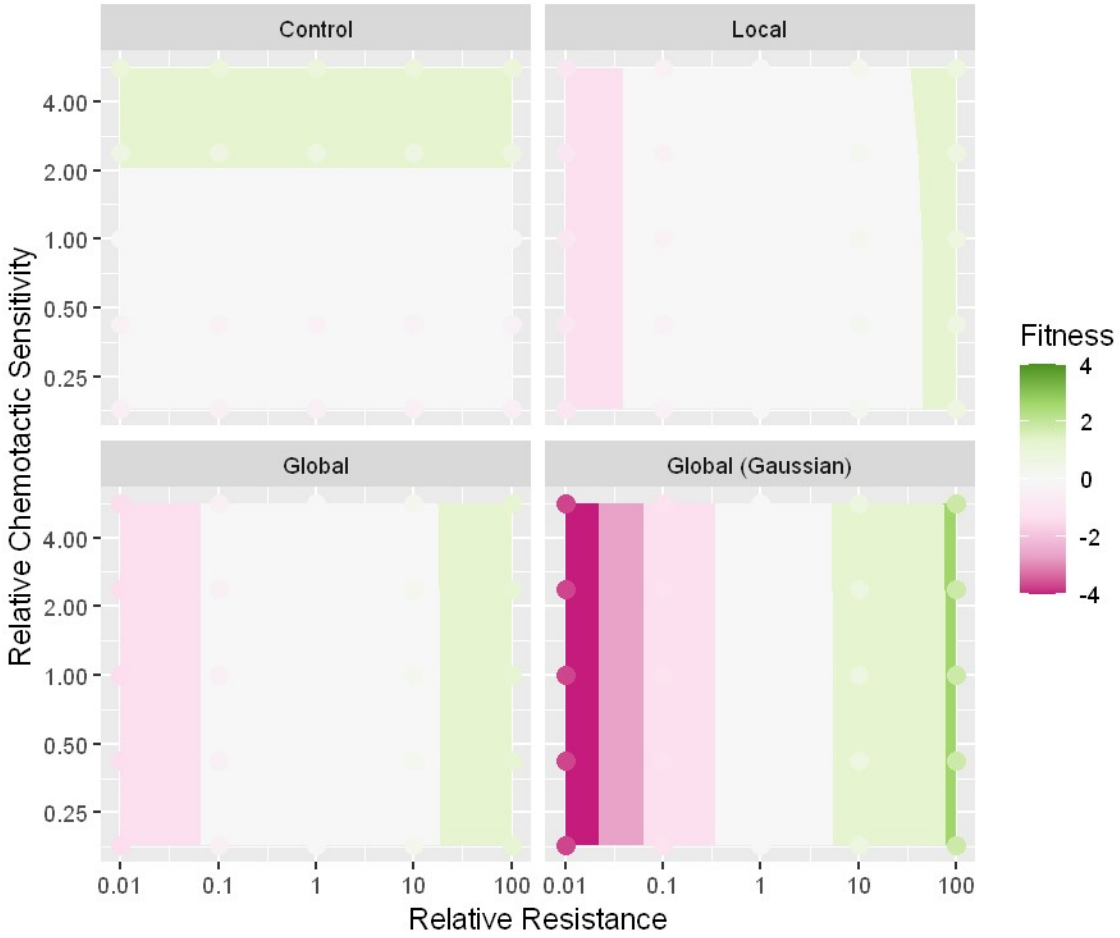

Fig S9. Parasite presence selects for host resistance and eliminates selection for host dispersal. *In silico* invasion experiments were carried out with a bacterial mutant that varied in its traits relative to the resident bacterial population, both competing in the presence of one of four different initial parasite spatial distributions. Each point is the result of a simulated invasion, colored by invader fitness = $\log_{10}$(final invader frequency/final resident frequency). Contours are interpolated for visualization.

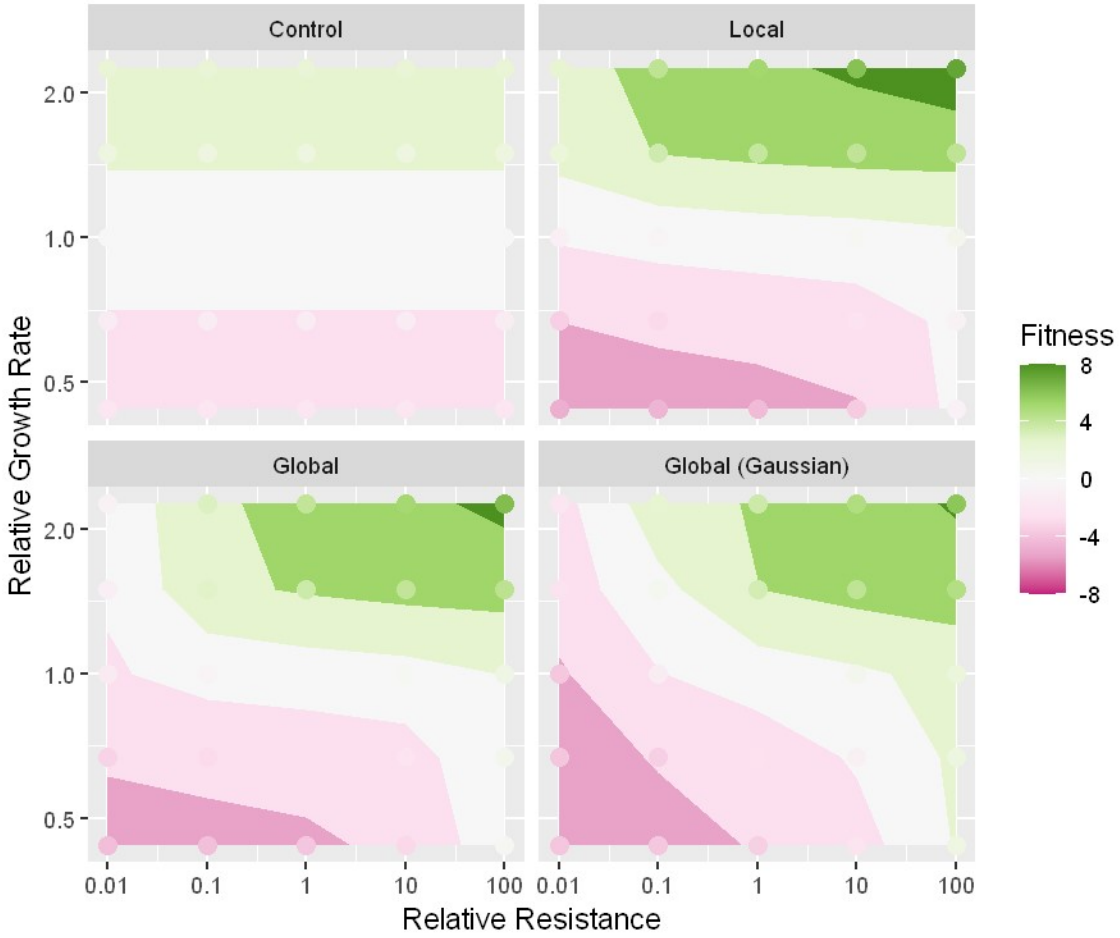

Fig S10. Parasite presence selects for host resistance and maintains selection for host growth rate. *In silico* invasion experiments were carried out with a bacterial mutant that varied in its traits relative to the resident bacterial population, both competing in the presence of one of four different initial parasite spatial distributions. Each point is the result of a simulated invasion, colored by invader fitness = $\log_{10}$(final invader frequency/final resident frequency). Contours are interpolated for visualization.

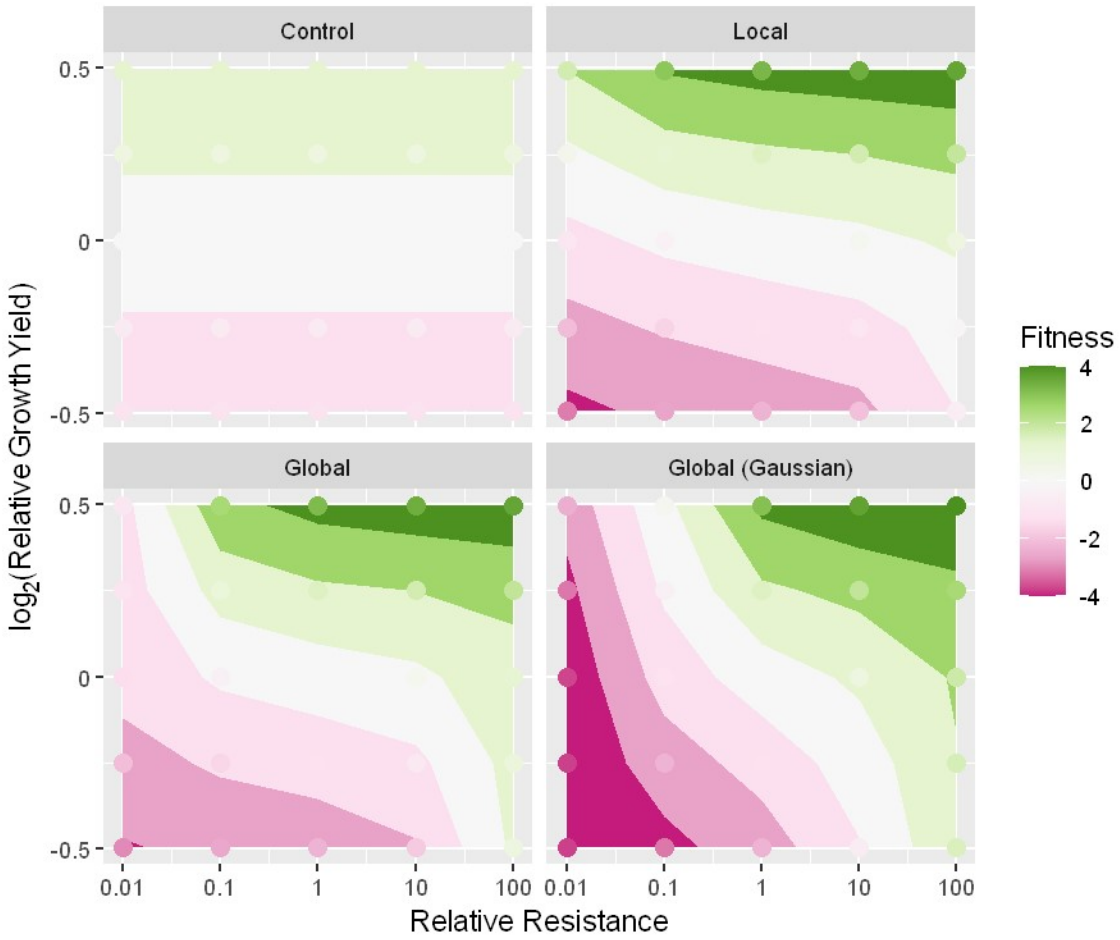

Fig S11. Parasite presence selects for host resistance and maintains selection for host growth yield. *In silico* invasion experiments were carried out with a bacterial mutant that varied in its traits relative to the resident bacterial population, both competing in the presence of one of four different initial parasite spatial distributions. Each point is the result of a simulated invasion, colored by invader fitness = $\log_{10}$(final invader frequency/final resident frequency). Contours are interpolated for visualization.

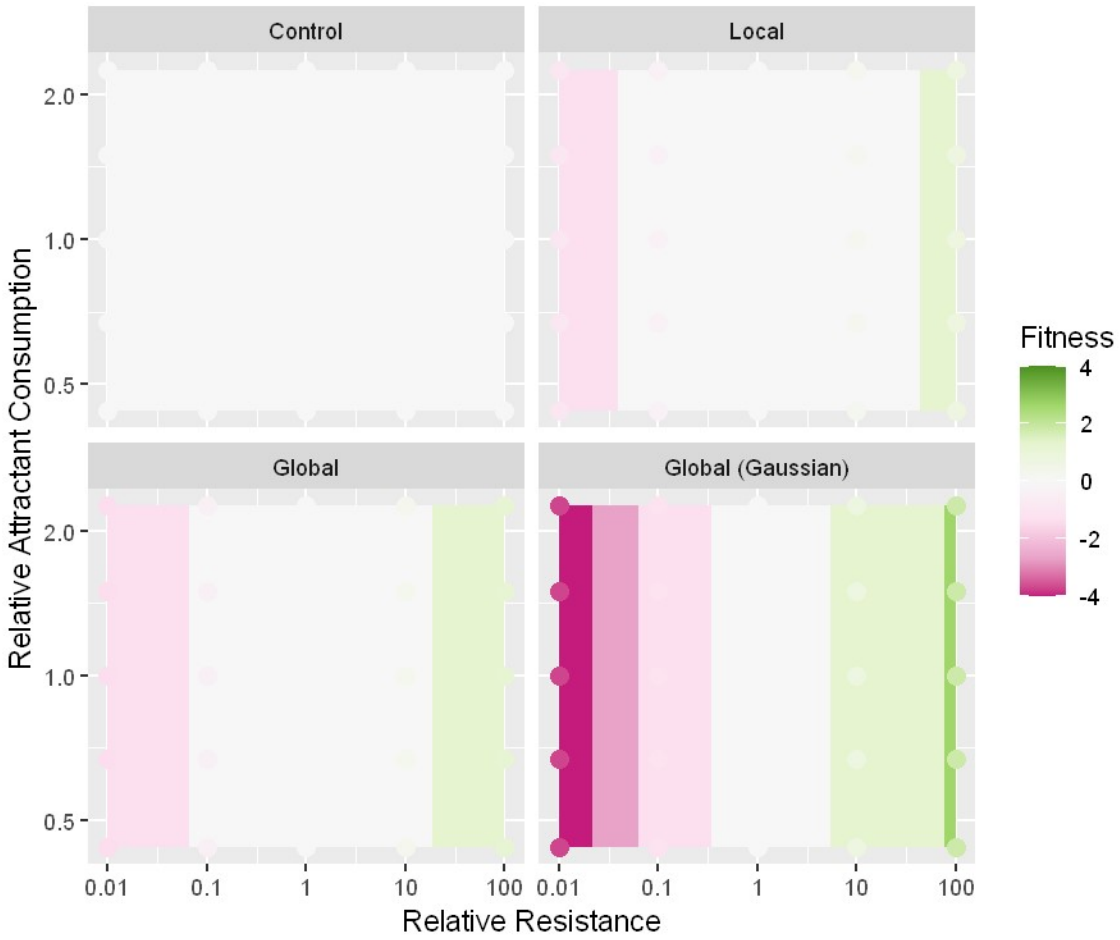

Fig S12. Parasite presence selects for host resistance with no effect on selection for host attractant consumption. *In silico* invasion experiments were carried out with a bacterial mutant that varied in its traits relative to the resident bacterial population, both competing in the presence of one of four different initial parasite spatial distributions. Each point is the result of a simulated invasion, colored by invader fitness = $\log_{10}$(final invader frequency/final resident frequency). Contours are interpolated for visualization.